Sensors & Actuators: B. Chemical 377 (2023) 133099

Contents lists available at ScienceDirect

Sensors and Actuators: B. Chemical

journal homepage: www.elsevier.com/locate/snb

Strategies to combat the fouling and surface texture issues associated with fabric-based colorimetric sensors

Peiyao Zhao [a], Evan D. Patamia [b], Trisha L. Andrew [a,b,*]

[a] Department of Chemical Engineering, University of Massachusetts Amherst, Amherst, MA 01003, USA
[b] Department of Chemistry, University of Massachusetts Amherst, Amherst, MA 01003, USA

ARTICLE INFO

Keywords:
Wearable sensors
Colorimetric detection
Antifouling
Chemical vapor deposition
Image processing

ABSTRACT

Colorimetric arrays are low-cost, portable options for numerous sensing applications and are bolstered by the possibility of using high-quality smartphone imaging for signal readouts. Despite advances in the use of colorimetric sensors in the biomedical, environmental, and food safety fields, reliable fabric-based colorimetric sensors for wearable applications have not yet been fully developed. There are two major issues that attenuate the sensitivity and selectivity of fabric-based wearable colorimetric sensors in comparison to their paper-based counterparts. First, wearable colorimetric sensors are subject to fouling by body oils and other biomolecules during wear. Second, fabric surfaces are highly rough and textured, which reduces the efficacy of portable imaging and complicates signal readout. In this work, a fabric-based colorimetric sensing platform is developed based on optimized chemistry and post-image processing. A colorimetric array on natural fabrics was created via sol-gel chemistry and encapsulated using photoinitiated chemical vapor deposition. This fabrication strategy yields sensors with robust color fastness, antifouling ability, fast colorimetric response, recoverability, and mechanical stability when it is exposed to a model gaseous analyte, ammonia. Moreover, it is found that the texture problem introduced by the fabric substrate can be mitigated by image pixel manipulation after the images are captured. The accuracy for classifying different pH levels by the fabric sensor array is improved after the image sharpening technique is applied. These successful demonstrations of both qualitative and quantitative analysis of vapor and aqueous solutions sensing illustrate the practical suitability of this fabric-based sensing platform, which is appealing to advanced wearable monitoring.

1. Introduction

Fabrics represent an appealing class of substrates for the development of smart sensors and sensing systems due to many advantages, such as high flexibility, large surface area, wear comfortability, lucrative and scalable production process [1,2]. Fabric-based biochemical sensors have grown rapidly for real-time tracking and clinical quality recording of biomarkers and essential physiological parameters, transforming daily modalities for healthcare monitoring [3]. Those sensors can incorporate optical, resistive, and capacitive sensing materials, enabling them to sense a variety of biochemical markers based on different mechanisms such as electrochemical [4,5], colorimetric [6,7], and optical sensing [8]. Unlike electrochemical sensors or e-Textiles that require many accessories, attachments and bulk electronics, the colorimetry-based sensor has gained increasing popularity in recent years, especially in point-of-care diagnostics. In principle, colorimetric sensing relies on the change in the absorbance and apparent color of a chromophore after the sensor is exposed to the target analyte, which can be registered visually by the naked eye or using a digital camera. The widespread interest in colorimetric devices is attributed to its non-invasive measurement, fast and naked-eye detection with low limits of detection [2,9,10]. When these devices are coupled with smartphone cameras, they can achieve on-site and real-time monitoring [11,12]. Despite these benefits, the commercialization of fabric-based colorimetric sensors has been impeded by many problems such as the lack of sensitivity, selectivity, and reversibility. Two major reasons for the low sensing performance have gone largely unaddressed in the literature: one is the issue of fouling and the other is sensitivity degradation due to fabric surface texture and roughness.

The issue of fouling is of high interest in electrochemical sensor development [13,14], but is comparatively neglected in the area of colorimetric sensors, especially sensors based on fabric substrates.

* Corresponding author at: Department of Chemical Engineering, University of Massachusetts Amherst, Amherst, MA 01003, USA.
E-mail address: tandrew@umass.edu (T.L. Andrew).

https://doi.org/10.1016/j.snb.2022.133099
Received 19 September 2022; Received in revised form 23 November 2022; Accepted 29 November 2022
Available online 1 December 2022

Contaminations such as drinks, food, body oils, and epidermal proteins are common interferents in wearable devices, limiting their use on fabric substrates in day-to-day use. These contaminants reduce the signal-to-noise ratio and cause false positive or negative results. One route to solve this issue is via the introduction of fluorine-containing polymer on fabric surface, which can change the surface wettability of the fabric substrate [15]. These coatings have low surface energy, which can resist the attachment of liquid contaminants and endow the surface of the fabric with antifouling ability [16,17].

In addition, the surface texture of the fabric substrate used in the sensor can affect the perceived color of the sample [18]. Mohammad et al. assessed seven different texture structures of dyed polyester yarn and showed that the fabric texture can perceptually and instrumentally influence the color quantity and quality [18]. Xin et al. [19] and Kandi and Tehran [20] investigated the effect of texture structures on the color differences. Based on those studies on surface textures and color attributes in large-scale textile industries, we are the first to propose that the surface textures might affect the colorimetric signal response of fabric-based sensors.

In this work, we built a colorimetric sensing platform using a chemical strategy to solve the issues with fouling and image post-processing to combat the complicating issue of surface texture on sensitivity. The problem with fouling was solved via encapsulating the colorimetric array with a thin, conformal coating of a fluorinated hydrophobic polymer using photoinitiated chemical vapor deposition (piCVD). We studied the liquid repelling activity and sensing response of the piCVD encapsulated array using ammonia as a model gaseous analyte, gauged changes to this response in the presence of contaminants and compared the performance of the encapsulated colorimetric array to its pristine, uncoated counterpart. We found that the strong hydrophobicity of the encapsulated sensor prevents the attachment of many liquids and preserves the functionality of the sensor. The problem of surface texture on the sensing performance is illustrated in the low classification accuracy of cotton lycra sample compared with a comparatively smooth and planar filter paper sample. To enhance the image quality, we processed the cotton lycra sample with image sharpening tools, which focused the soft edges in the image. The sharpening effect produced an enhanced intensity differences on different images and hence, increased the clarity both visually and instrumentally.

2. Materials and methods

2.1. Materials

Phenolphthalein, Methyl red, Methyl orange, Bromothymol blue, Thymol blue, (3-glycidyloxypropyl)trimethoxysilane (GPTMS), tetraethyl orthosilicate (TEOS), sodium acetate trihydrate, sodium phosphate monobasic, sodium phosphate dibasic, ethanol, ammonia hydroxide solution (28–30 %), 2-hydroxy-2-methylpropiophenone (HMPP), 3,3,4,4,5,5,6,6,7,7,8,8,8-tridecafluorooctyl acrylate (TFOA), bovine serum albumin (BSA) were purchased from MilliporeSigma and TCI America and were used without purification. Milk, coffee, and olive oil were purchased from the local grocery store. Silicon wafer and scoured cotton, cotton lycra, and filter paper were used as substrates.

2.2. Preparation of chemoresponsive dye arrays

We used a modified method to deposit the sol-gel doped chemo-responsive dyes on the substrate surface [21]. 0.55 mL TEOS, 1.6 mL water, and 2.5 mL ethanol were first mixed, followed by 12.5 mg sodium acetate trihydrate, to hydrothermally form a silicate network. Next, 0.2 mL GPTMS was added to serve as a covalent linking point for small molecules dyes. Finally, three different dyes or dye mixtures were added into the silicate solution: Methyl red, bromothymol blue and universal indicator (phenolphthalein, methyl red, methyl orange, bromothymol blue, thymol blue). The amount of dye added was 20 mg. The mixture was vigorously stirred for 30 min on a magnetic stir plate at 50 °C. Fabric substrates were cut into 2.5 × 2.5 cm^2 dimensions. 2 μL of each of the above dye/sol-gel solutions was drop-casted onto the cotton surface and cured at 100 °C overnight.

2.3. Encapsulation of chemo-responsive dye arrays

To prepare the polymer film, photoinitiated chemical vapor deposition (piCVD) of TFOA on fabric-based chemo-responsive dye arrays and silicon wafer (as a reference for characterization) were conducted in a home-made stainless-steel wall reactor (290 mm diameter and 70 mm height). Substrates were put at the center of the reactor. Photoinitiator HMPP and monomer TFOA were pre-heated to 110 °C in the glass ampule via the heating tape. A UV-lamp with 254 nm intensity (UVP, UVLS-24 EL Series, 4 W) was switched on after the monomer TFOA and photoinitiator was introduced into the chamber through the articulated needle valves and the base pressure of the reactor was maintained at 200 mTorr. The deposition proceeded for 5 min and was followed by vacuum annealing step to pull out unreacted monomers and photoinitiator from the film deposited on the substrate surface. This procedure of piCVD encapsulation was previously introduced in our published paper [22].

2.4. Characterization of surface coating

Fourier transform infrared spectroscopy (Bruker Alpha) of the polymerized TFOA (pTFOA) coatings on the reference silicon wafer was measured. Contact angles of water on the sample were measured by a contact angle goniometer (One Attension). The thickness of the pTFOA films created by piCVD was measured using a combination of atomic force microscopy (AFM, Bruker), a Dektak profilometer and spectroscopic ellipsometry. Fourier-transform ion cyclotron resonance mass spectrometry (Bruker SolariX) was used to measure the spectrum of the TFOA, solvent blank (50 % acetonitrile), the washing solution of colorimetric sensor, and the washing solution of pristine cotton under identical conditions. TFOA was diluted to ca. 10 μM in 50 % acetonitrile, an equal volume of acetonitrile was added to an aliquot of each washing solution.

2.5. Colorimetric ammonia sensing

The aqueous Ammonium hydroxide (NH_4OH), an ammonia solution of water, was used to generate the ammonia gas via evaporation, according to Eq.(1). The molar amount of ammonia hydroxide is equal to the molar amount of ammonia gas. Different volumes of ammonium hydroxide solution (10uL, 20uL, 30 u, 40 uL, 50 uL) were injected into petri dishes, respectively. Sensors were taped to the inside surface of a petri dish cover and the cover then inverted over the petri dish to create a mostly-closed system. In this mostly-closed system, ammonia reaches a gas-solution equilibrium. Care was taken to ensure that the sensor did come into physical contact with the ammonium hydroxide solution in the petri dish. The calculation of ammonia gas concentration in the mostly-closed system is shown in the following Eq.(2)[23]. We provided one example calculation for the preparation of ammonia gas from the ammonia hydroxide solution in the Electronic Supplementary Material. The samples were taken out after 10 min and imaged using a flatbed scanner (CanoScan LiDE300). The calculation equation for limit detection is shown in Eq.(3).

$$NH_4OH\ (aq) \rightarrow NH_3\ (g) + H_2O\ (aq) \quad (1)$$

$$C_{ppm} = \frac{V \times D}{M \times V'} \times 2.4 \times 10^4 \quad (2)$$

V-the volume of ammonia hydroxide solution, uL

D-the density of the ammonia hydroxide solution, 0·45 g/mL

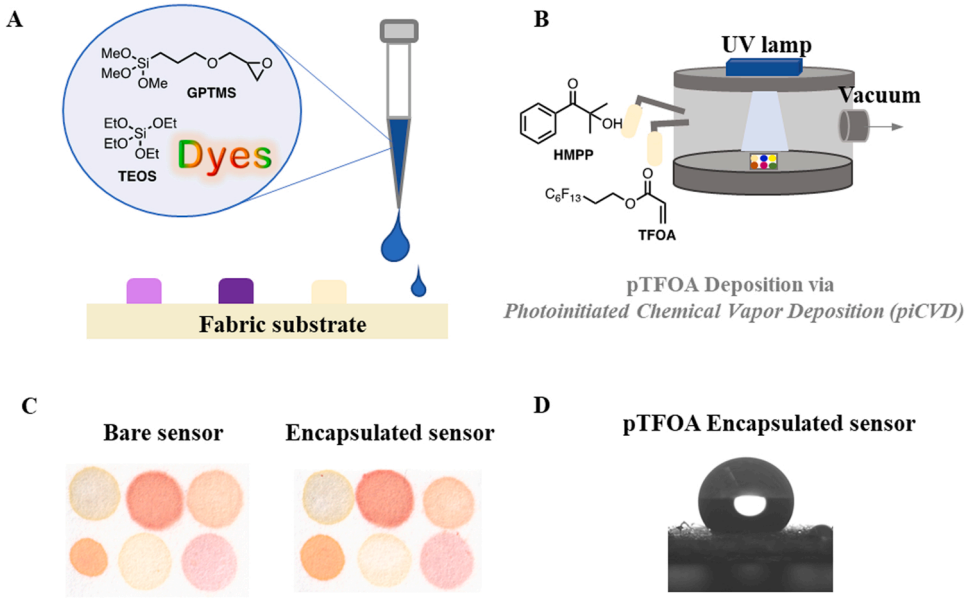

Fig. 1. A. Schematic illustration of sol-gel immobilization of dyes on fabric substrate. B. Summary of the photoinitiated chemical vapor deposition process used to encapsulate the colorimetric bare sensor. C. Optical images of encapsulated sensor and bare sensor. D. Static water contact angle measurements of pTFOA encapsulated sensor surface, using 5 μL of deionized water.

M-molecular weight of the ammonia hydroxide, 35·5 g/mol

V- the total volume of the petri dish, 157 cm^3

$$LOD = \frac{3.3 \times standarddeviationof theintercept}{absolutevalueof theslope} \quad (3)$$

2.6. Anti-fouling tests

Readily-available BSA was used as a model biomolecule to simulate surface fouling upon wear. The sensor was immersed in a 10 mM BSA aqueous solution, followed by subsequent washing with deionized water. The washing solution and the sensor were characterized using two different UV–visible spectrophotometers (Agilent and ThermoFisher Evolution 220, respectively). For comparison, the same experiment was done on the intrinsic cotton substrate. In addition, to demonstrate that the developed sensors' colorimetric ammonia sensing response would not be influenced by the presence of diverse liquid foulants, different solutions including milk, coffee, and olive oil were dropped onto the sensor surface. The sensors were then taken inside petri dishes for colorimetric ammonia sensing.

2.7. Humidity resistance and mechanical stability

The colorimetric sensor was placed in a home-made airtight vapor black box, depicted in Figure S1 in the Electronic Supplementary Material. 1 mL ammonia hydroxide solution was injected into the petri dish inside the black box to generate the ammonia gas. A miniature fan was used to disperse the gas throughout the entire box. The humidity level inside the box was controlled by injection of nitrogen gas and droplets of boiling water. The humidity and temperature were measured continuously via a hygrometer (ThermoPro TP50). The image was captured by a raspberry pi camera and further processed on MATLAB (R2020a). The sensor's mechanical stability was determined through the comparison of the ammonia sensing response before and after the abrasion. Abrasion test was performed by putting the sensor on the sandpaper and sliding a 1 kg calibration weight on the sensor surface.

2.8. Color parameters and statistical image analysis

The images of sensors exposed to ammonia and aqueous solution of different pH levels were imported to MATLAB and the region of interest (ROI) of each dye spot on the sensor surface was segmented from the background. For images of ammonia sensors, the average hue intensity was extracted from the ROI and applied to detect the color change of the sensor. For images of aqueous solution, images before and after the sensors exposed to the water solution (pH = 4,5,6,7,8) were taken and a difference map was generated via subtracting the before image from the after image. RGB color space was used, and each image is represented by 33 color vectors (each image contains 11 dye spots and each spots have 3 color intensity channels-red(R), blue(B), and green(G)). This matrix of data is evaluated by principal component analysis (PCA) and hierarchical clustering analysis (HCA). PCA plot and dendrogram are produced for visualizing the result. The total Euclidean distance (TED) is calculated via the following equation:

$$TED = \sqrt{(R_{before} - R_{after})^2 + (G_{before} - G_{after})^2 + (B_{before} - B_{after})^2}$$

3. Results and discussion

3.1. Preparation of chemoresponsive dye arrays

A colorimetric array on paper and fabric substrates was created using previously-reported sol-gel chemistry [22,24]. The schematic for this process is shown in Fig. 1A. The sol-gel process involved the alkoxysilane precursor which underwent a hydrolysis and subsequent polymerization reaction to generate the sol. Chemo-responsive dyes were embedded into the sol-gel solution and the entire solution was drop-casted on fabric substrate. Meanwhile, the addition of sodium electrolyte in the solution neutralized the negative charges of the cellulosic substrate and enhanced the dye adsorption. This process imparted fabric substrate with color fastness and wash stability.

Once the dye-encapsulated silica sols were patterned onto the desired substrate surface and cured, piCVD was used to create thin and conformal polymer encapsulations, the schematic of which is illustrated in Fig. 1B. This process is solvent-free and can be operated under low vacuum and low temperature conditions to generate a thin film on the

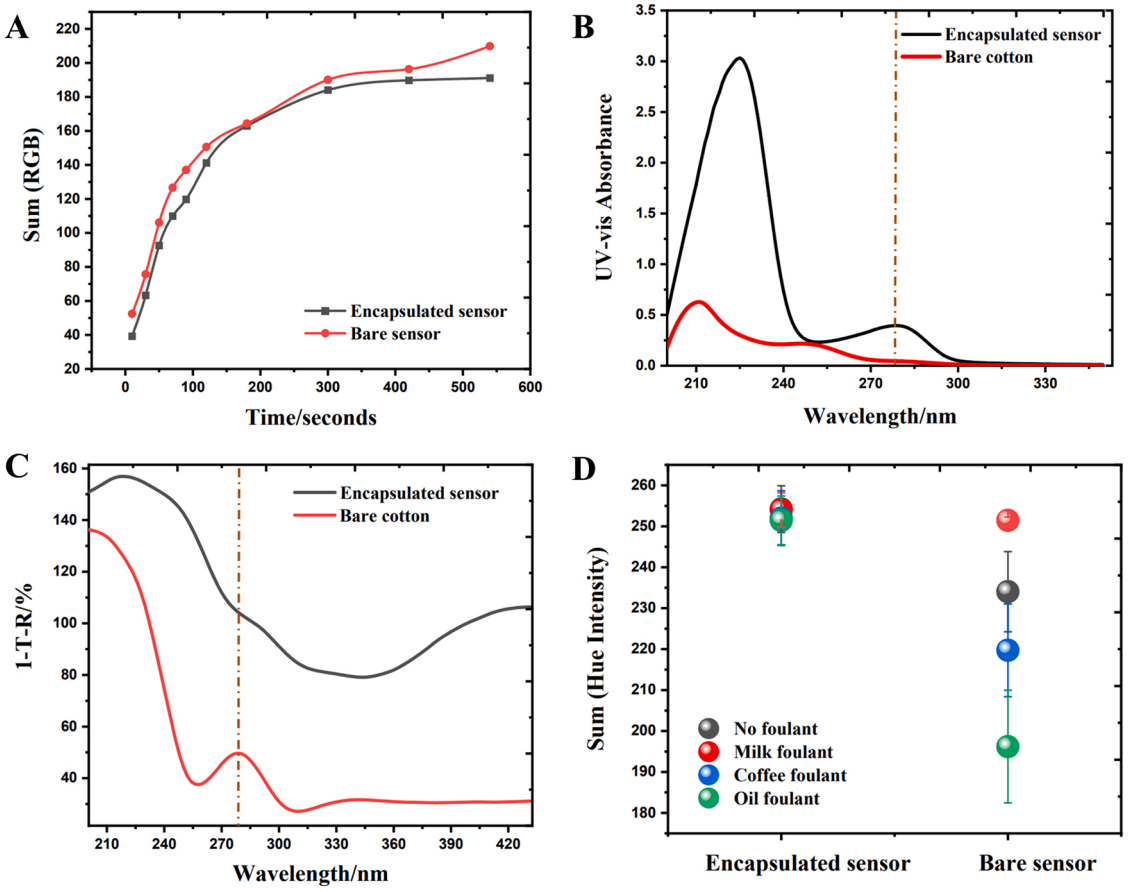

Fig. 2. A. The temporal change of total summation of red, green, and blue intensity of the encapsulated sensor and bare sensor after exposing to the same amount of ammonia. B. UV–vis spectroscopy of the washing solution of the encapsulated sensor and bare cotton immersed in the BSA. C. 1-T-R measurement of the encapsulated sensor and bare cotton immersed in BSA. D. Total Hue intensity change of the encapsulated sensor and the bare sensor (cotton with sol-gel immobilized dyes) after being fouled by milk, coffee, and olive oil.

substrate surface without modifying the functional groups of the monomer precursor [25,26]. Previous studies have shown that the deposition of thin fluoropolymer films via iCVD and piCVD is a highly effective method to render various natively-hydrophilic surfaces hydrophobic [27,28]. We posited that a hydrophobic coating could minimize the nonspecific binding and attachment of the interferents and, thus, prevent sensor fouling and mitigate the signal loss during continuous real-time sensing. In our piCVD process, the silicon wafer was placed alongside the sensor sample and coated with pTFOA for the reference. The vaporized monomers TFOA and photoinitiator were fed into the reaction chamber. At the UV wavelengths of 254 nm, the photoexcited carbonyl species are decomposed into radicals and initiated a free-radical polymerization [22,29]. In Fig. S2, the band at 1637 cm^{-1}, assigned to the stretching frequency of the unsaturated acrylate C=C bond in the TFOA monomer, did not appear in the FTIR spectrum of the film isolated on the silicon wafer surface, which confirmed that the TFOA monomer was fully polymerized during piCVD to form pTFOA. The narrow absorbance at 3200 cm^{-1} was attributed to a small amount of adsorbed moisture on the substrate due to the humidity of our lab space. The typical stretching peak of CF_2 and CF_3 were also observed at 1100–1250 cm^{-1} [30], verifying the retention of the fluorinated moiety after the vapor deposition.

The apparent/perceived weight, observable color and surface texture, and handfeel of the bare sensors did not change after piCVD encapsulation, as shown in Fig. 1C. The measured weight of the sensors increased by less than 0.1 mg after piCVD encapsulation. Similar to previous reports [22,27]. the thickness of the pTFOA coating was approximately 300 nm on the reference silicon wafer, although the pTFOA coating on a silicon wafer is highly nonuniform and forms droplet-like islands due to expected epitaxial mismatching and surface wetting problems. Nonetheless, informed by previous studies [22,27], we expected that even a nonuniform pTFOA coating on fabric and paper substrates would render the samples hydrophobic. As seen in Fig. 1D, the static contact angle of the encapsulated colorimetric sensor was 145°. The fluorinated polymer coating displayed a low surface energy and low wettability, and hence a high contact angle, transforming the cotton surface from hydrophilic to hydrophobic.

While certain highly-fluorinated small molecules, such as perfluorooctanoic acid (PFOA) and perfluorooctanesulfonic acid (PFOS), that are used in fabric treatments have been proven to be bioaccumulative once they are leached into the environment [31], we established that the pTFOA on our sensor surface is robust and that no leachable fluorinated residues were left on the sensor surface after fabrication. As shown in Figure S3, the mass spectrum of the washing sample of the sensor showed no apparent peak correlated with TFOA. In addition to the fact that pTFOA is not soluble in water, all of those suggest that there is no biohazard in our colorimetric sensor.

3.2. *Effects of encapsulation on sensing response*

We used ammonia as a model gas to probe the effect of the pTFOA encapsulation on the colorimetric output of the sensor. We chose ammonia gas due to its easy preparation and accessibility, and because the small and polar ammonia molecule displays high transport mobility (and can thus sample multiple surface sites) while also being susceptible to strong ionic and hydrogen bond interactions that can pin the molecule

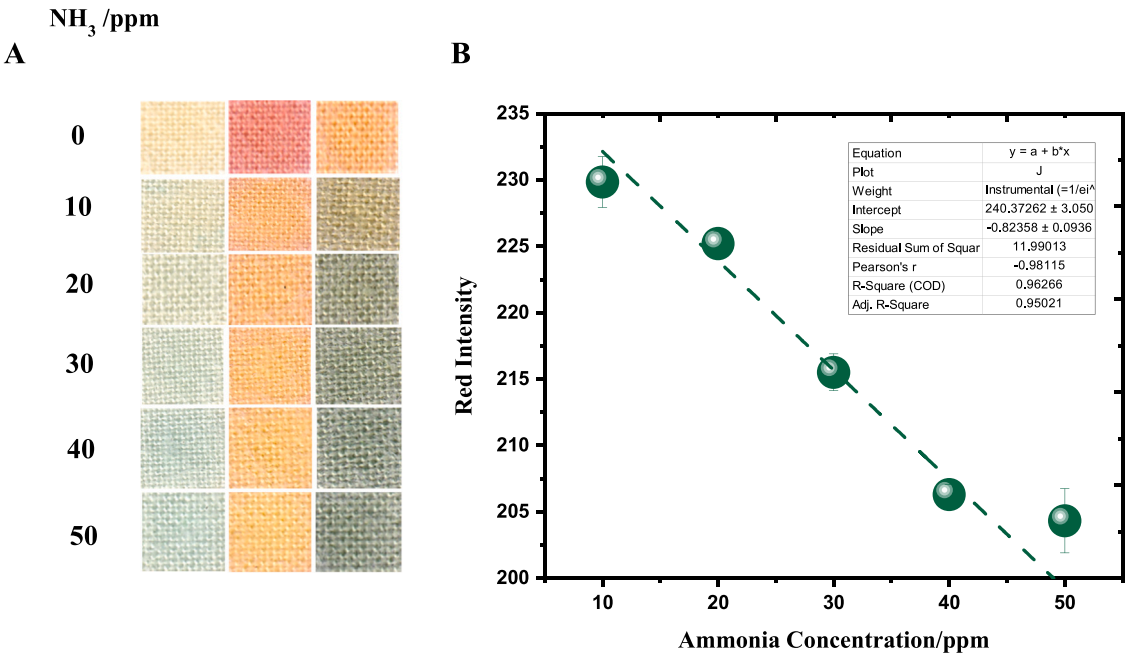

Fig. 3. A. Optical image of dye spots on the encapsulated sensor after response to increasing concentrations of ammonia gas (from left to right: bromothymol blue, universal indicator, methyl red). B. Calibration plot with error bar of the ammonia concentration change (Y axis represents the red intensity from the bromothymol blue indicator, X axis represents the ammonia concentration in ppm).

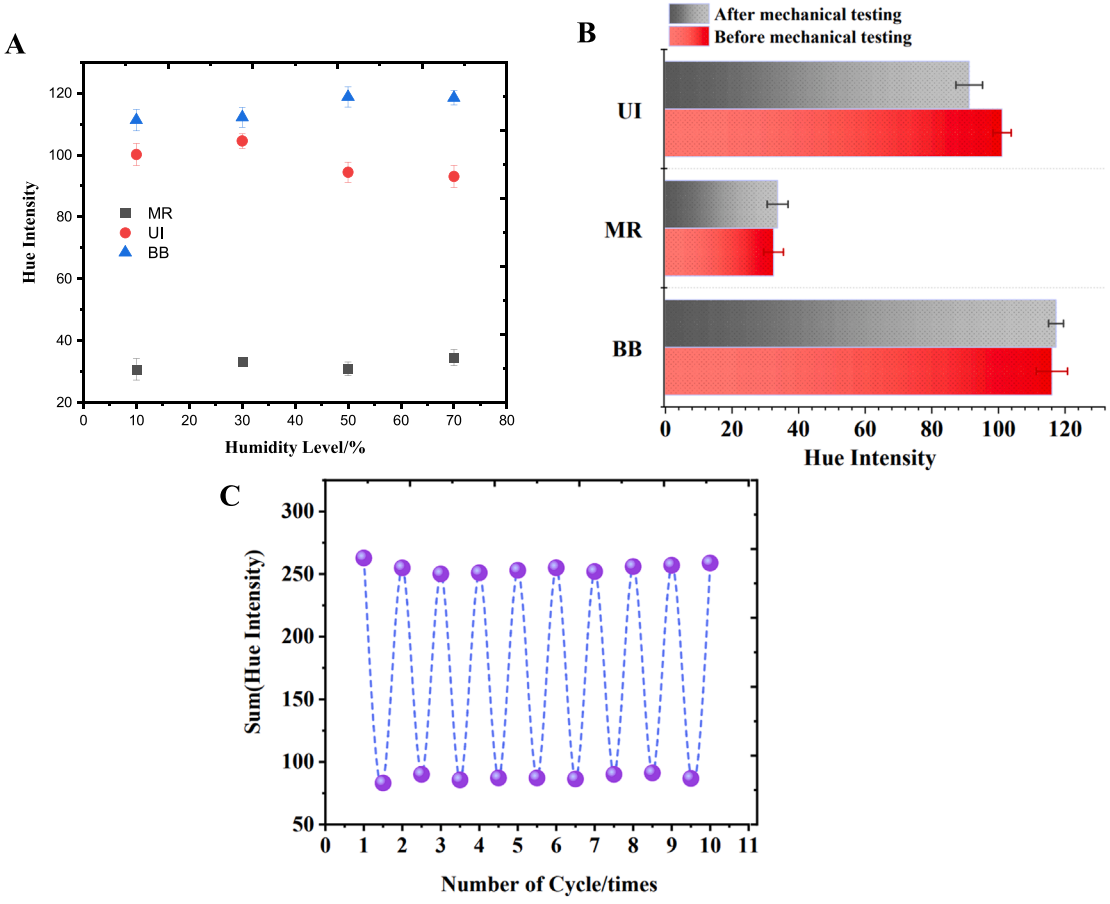

Fig. 4. A. Humidity test. B. Mechanical stability test, and C. Color recoverability of the encapsulated sensor. (BB, UI, MR represent bromothymol blue, universal indicator, and methyl red).

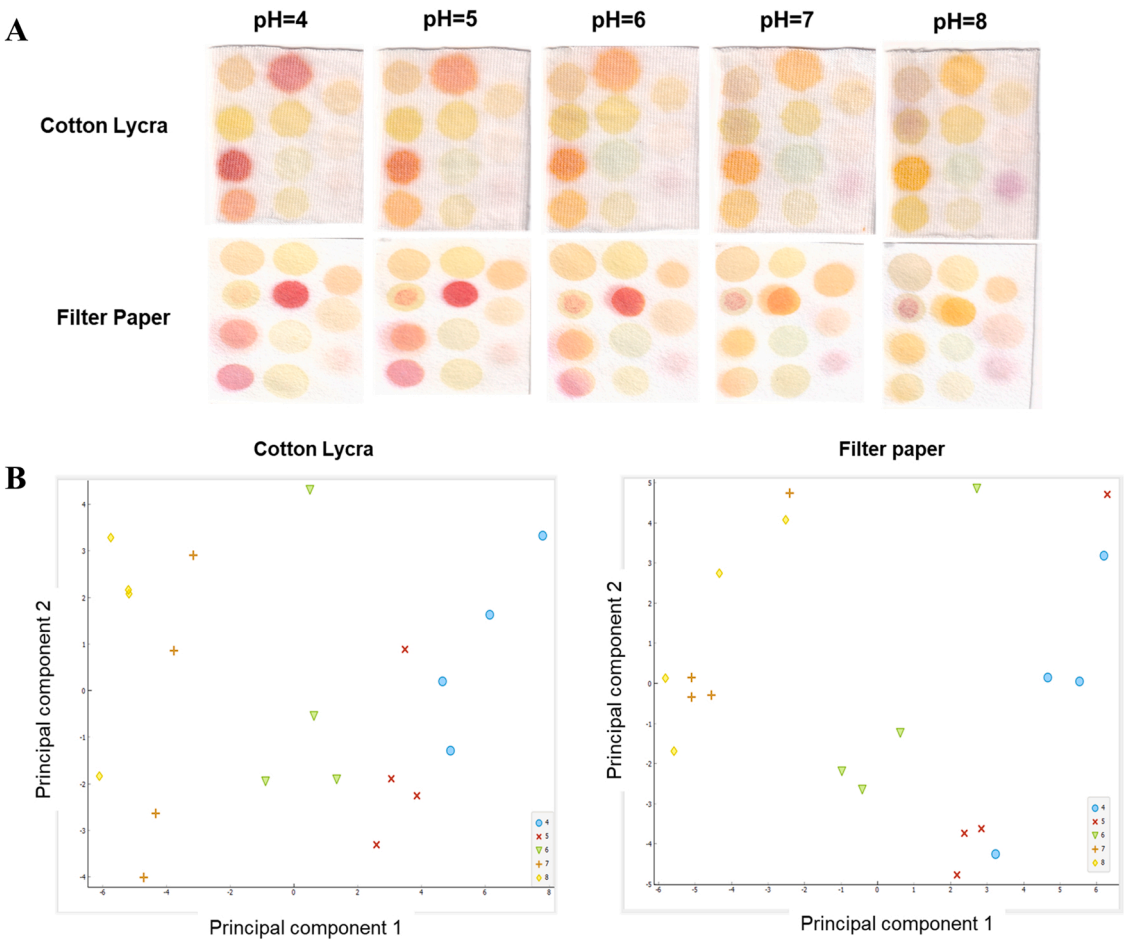

Fig. 5. A. Optical images of original cotton lycra-based sensor and filter paper-based sensor after their exposure to 5 different pH levels. B. PCA plots of the data sets from cotton lycra-based sensor and filter paper-based sensor.

to random sites on the sensor. As shown in Fig. 2A, the encapsulated sensors performed comparable to bare sensors when exposed to the same amounts of ammonia. The temporal response of the RGB color changes of bare and encapsulated sensors were almost identical, indicating that the thin encapsulation created using piCVD did not hinder mass transport of target analytes to the underlying active layer. Moreover, the hue change of each spot on the encapsulated sensor and bare sensor surface was almost identical after ammonia detection, as indicated in Figure S4. This observation confirmed that the chemoresponsive dyes maintained their color changing ability after piCVD encapsulation, suggesting that the piCVD process did not bleach or otherwise chemically damage the active chromophores in the colorimetric sensor.

3.3. *Antifouling ability of the encapsulated sensor*

The antifouling ability of the encapsulated sensor was evaluated using BSA. We chose BSA because it is a readily available model of biomolecules that represents a more complex biological system which can cause stronger fouling issues to surfaces such as fabrics [32–34]. Fig. 2B shows that the washing solution of the sensor exhibited a peak at 280 nm on UV–vis spectroscopy, which is the typical absorption peak for BSA [35]. However, almost no peak corresponding to BSA was observed from the washing solution of the pristine cotton substrate, likely because the protein is strongly absorbed onto the pristine cotton and cannot easily be washed off. Additionally, as shown in Fig. 2C, the presence of the characteristic absorption peak of BSA on the solid-state 1-T-R (Absorbance = 1 – Transmittance − Reflectance) spectrum of bare cotton substrate surface suggested that the protein accumulates on the cotton surface, while the encapsulated colorimetric sensor did not exhibit similar peaks in its 1-T-R spectrum because the protein solution was effectively repelled from the hydrophobic surface.

To further demonstrate that the encapsulated sensor could repel diverse foulant solutions and maintain its gas sensing ability, several droplets of milk, coffee and olive oil were added onto the sensor surface. Those droplets did not spread on the sensor surface and, instead, they began to bead up into spheres that could simply be brushed off the sensor. The entire colorimetric sensor remained dry and did not soak up the liquid droplets that sat on its surface for upwards of 30 min. As illustrated in Fig. 2D, for the encapsulated colorimetric sensor, the summation of hue intensity for non-fouled sensor and fouled sensor were almost equivalent after the ammonia exposure. On the contrary, those liquids could easily wet the surface of the bare sensor, which lacked the pTFOA encapsulation, and immediately soaked into the entire sensor due to the capillary effect and caused significance signal changing during ammonia sensing, indicated by large intensity difference between the bare sensors fouled by those liquids and that without any foulant.

3.4. *Detection of ammonia with the encapsulated sensor*

Aside from the antifouling property, we proved that the developed sensor could achieve a practical functionality, namely, the sensitivity and stability like other colorimetric sensors [36]. Gaseous ammonia was continued to be used as a model analyte. In Fig. 3A and B, the summation of red intensity of three-color spots on the sensor exhibited a gradient change after they were reacting with different ammonia concentrations

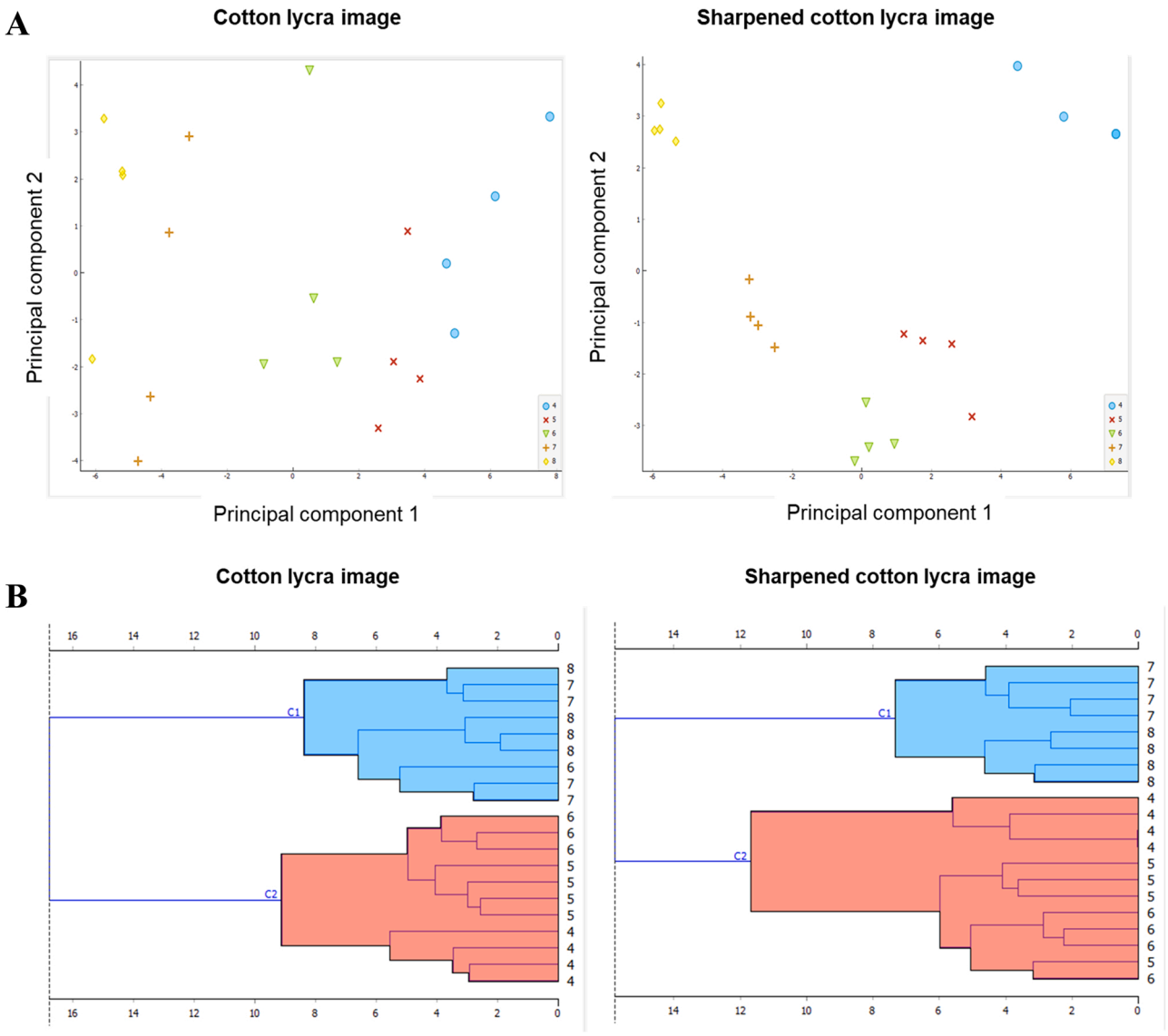

Fig. 6. A. PCA plots of the data sets from the cotton lycra-based sensor and cotton lycra-based sensor after sharpening. B. Dendrograms of the data sets from the cotton lycra-based sensor and cotton lycra-based sensor after sharpening.

due to the deprotonation of the indicators. This provided semi-quantitative information about the approximate amount of ammonia in the air. The limit of detection for ammonia detection calculated from this method is 52.98 ppm. Most sensitive dyes are susceptible to humidity variation, which can compromise the detection accuracy of a colorimetric sensor [36]. Thanks to the pTFOA coating, the sensor is immune to humidity change at different levels, as shown in Fig. 4A. Meanwhile, in Fig. 4B and C, the sensor exhibited mechanical robustness after abrasion and fast reversibility after repetitive cycles.

3.5. *Combating texture issues during digital imaging*

Another issue that complicates the signal readout of fabric-based colorimetric sensors device is the surface texture of knit and woven fabrics. Unlike the filter paper, which has a much flatter and two-dimensional (2D) surface structure, most daily wear fabrics, such as knitted cotton lycra, have comparatively complicated surface topologies that are captured by all high-quality imaging systems, including smartphones. Therefore, we sought to compare the difference of a three-dimensional textile surface to a 2D analog in the context of colorimetric image sensing.

To investigate this issue, we fabricated a multidimensional sensor array comprised of eleven distinct sensing spots. The sensing spots contained eleven different pH responsive chromophores and were deposited on the surface of various substrates using the same sol-gel chemistry described earlier. pH sensing and pH responsive dyes were pursued for this part of the study (instead of ammonia sensing) because we had access to a much larger set of known pH sensitive dyes with a broad range of RGB and hue intensity responses to pH. The piCVD encapsulation step was intentionally omitted for this part of the study to allow aqueous solutions of varying pH to wet/soak the sensors. Knitted cotton lycra and filter paper were particularly chosen as substrates to represent a significantly textured and a comparatively flat surface, respectively.

pH discrimination was investigated for pH units ranging from pH 4–8 for five replicates of each substrate in total (Fig. 5A). Before proceeding with any image analyses, we ensured that the sensor arrays lacking a piCVD encapsulation were colorfast upon exposure to aqueous solutions of pH from 4 to 8 and could be used for aqueous analyte detection in this section. The combination of different indicators into one dot on an array allowed an enlarged difference between adjacent pH values and higher image resolution. After taking the images, 33 vectors were extracted

from each sensor array and fed into principal component analysis (PCA) and hierarchical clustering analysis (HCA) algorithms. HCA is a technique to build a dendrogram to represent the data; the dendrogram is a type of tree diagram showing the relationship between similar data. PCA processed and reduced the high dimensional data matrix to two principal components and visualized them on a two-dimensional cartesian coordinate system. Fig. 5B shows the PCA plot of the data matrix obtained from the cotton lycra-based sensor and a Whatman filter paper-based sensor. The filter paper-based sensor showed well-separated clusters for each of the pH level, however, separation was not as clear on the cotton lycra. Since the same fabrication and imaging procedure were applied to both cotton lycra and the filter paper-based sensor, we suspected that the biggest reason for their difference in classification accuracy is the complications and scattering introduced by knitted texture of the lycra. In order to enhance the color difference between each image, we applied a filter on all the images to extract the edge noise, followed by a sharpening tool to reduce blur. These processing steps were performed in Adobe Photoshop. Fig. 6A shows a comparison of the PCA plots extracted from the lycra sensor before and after image sharpening, showing clear separation between each pH groups in the sharpened sample images. Meanwhile, the dendrogram, which shows the similarities and dissimilarities of each group data, were obtained from the HCA. Clades that are close to the same height are similar to each other. In Fig. 6B, there were some misclassifications between data of pH 6, pH 7, and pH 8 in the dendrogram of cotton lycra-based sensor while only one misclassification of pH 5 were observed in that of sharpened image. These observations indicated that image processing can be used to practically solve the textile texture issue in digital imaging of fabric-based colorimetric sensors.

4. Conclusion

In this study, we set out to solve the fouling and surface texture issues that need to be addressed in order to promote colorimetric fabric-based sensing. The vapor deposition technique is used to coat a hyperbranched fluorinated polymer layer on a daily-wear fabric, endowing it with strong anti-fouling properties while maintaining the sensor's original sensing response. Our method proves to be safe and non-hazardous as the fabricated sensor shows no residue of monomer and no leaching of polymer into water. We also develop a method to combat the sensitivity issues that textured surfaces such as fabrics can present. With an image sharpening algorithm, we can maximize the sensor's clarity and enhance the precision of the device. Our strategy proves to be the first one to solve the fouling issue of colorimetric solid-substrate sensors and to improve the image classification efficiency via image processing techniques. More work will be carried out in the future research regarding the synthesis of non-fluorinated polymer using piCVD to fabricate antifouling surfaces and more advanced computational imaging techniques to improve signal detection performance. Overall, we report methods to combat the fouling and texture issue in fabric-based colorimetric sensors and those advances can lead to the development of fabric arrays on the mask that are sensitive and wear-resistant for extended hours or even days.

CRediT authorship contribution statement

Peiyao Zhao: Conceptualization, Data curation, Methodology, Software, Writing-original draft&review&editing. **Evan Patamia**: Software, Writing-Review and Editing. **Trisha L. Andrew:** Methodology, Funding acquisition, Project administration, Writing-Review&editing.

Declaration of Competing Interest

The authors declare that they have no known competing financial interests or personal relationships that could have appeared to influence the work reported in this paper.

Data availability

Data will be made available on request.

Acknowledgments

This work was funded by a generous gift from the Sarah Hawes Trust to T.L.A. and the University of Massachusetts Department of Chemistry.

Appendix A. Supporting information

Supplementary data associated with this article can be found in the online version at doi:10.1016/j.snb.2022.133099.

References

[1] I.I. Shuvo, A. Shah, C. Dagdeviren, Electronic textile sensors for decoding vital body signals: state-of-the-art review on characterizations and recommendations, Adv. Intell. Syst. 4 (2022), 2100223, https://doi.org/10.1002/aisy.202100223.
[2] A. Sharma, A. Singh, A. Khosla, S. Arya, Preparation of cotton fabric based non-invasive colorimetric sensor for instant detection of ketones, J. Saudi Chem. Soc. 25 (2021), https://doi.org/10.1016/j.jscs.2021.101340.
[3] A.J. Bandodkar, P. Gutruf, J. Choi, K. Lee, Y. Sekine, J.T. Reeder, W.J. Jeang, A.J. Aranyosi, S.P. Lee, J.B. Model, R. Ghaffari, C.-J. Su, J.P. Leshock, T. Ray, A. Verrillo, K. Thomas, V. Krishnamurthi, S. Han, J. Kim, S. Krishnan, T. Hang, J.A. Rogers, Battery-free, skin-interfaced microfluidic/electronic systems for simultaneous electrochemical, colorimetric, and volumetric analysis of sweat, 2019. ⟨https://www.science.org⟩.
[4] X. Liu, P.B. Lillehoj, Embroidered electrochemical sensors for biomolecular detection, Lab Chip 16 (2016) 2093–2098, https://doi.org/10.1039/c6lc00307a.
[5] A. Piper, I. Öberg Månsson, S. Khaliliazar, R. Landin, M.M. Hamedi, A disposable, wearable, flexible, stitched textile electrochemical biosensing platform, Biosens. Bioelectron. 194 (2021), https://doi.org/10.1016/j.bios.2021.113604.
[6] X. Yue, F. Xu, L. Zhang, G. Ren, H. Sheng, J. Wang, K. Wang, L. Yu, J. Wang, G. Li, G. Lu, H.-D. Yu, Simple, skin-attachable, and multifunctional colorimetric sweat sensor, ACS Sens. (2022), https://doi.org/10.1021/acssensors.2c00581.
[7] J. Xu, X. Tao, X. Liu, L. Yang, Wearable eye patch biosensor for noninvasive and simultaneous detection of multiple biomarkers in human tears, Anal. Chem. (2022), https://doi.org/10.1021/acs.analchem.2c00614.
[8] M. Caldara, C. Colleoni, E. Guido, V. Re, G. Rosace, Optical monitoring of sweat pH by a textile fabric wearable sensor based on covalently bonded litmus-3-glycidoxypropyltrimethoxysilane coating, Sens Actuators B Chem. 222 (2016) 213–220, https://doi.org/10.1016/j.snb.2015.08.073.
[9] N. Promphet, P. Rattanawaleedirojn, K. Siralertmukul, N. Soatthiyanon, P. Potiyaraj, C. Thanawattano, J.P. Hinestroza, N. Rodthongkum, Non-invasive textile based colorimetric sensor for the simultaneous detection of sweat pH and lactate, Talanta 192 (2019) 424–430, https://doi.org/10.1016/j.talanta.2018.09.086.
[10] D.H. Kim, J.H. Cha, J.Y. Lim, J. Bae, W. Lee, K.R. Yoon, C. Kim, J.S. Jang, W. Hwang, I.D. Kim, Colorimetric dye-loaded nanofiber yarn: eye-readable and weavable gas sensing platform, ACS Nano 14 (2020) 16907–16918, https://doi.org/10.1021/acsnano.0c05916.
[11] O. Adeniyi, P. Mashazi, Kirigami paper-based colorimetric immunosensor integrating smartphone readout for determination of humoral autoantibody immune response, Microchem. J. 178 (2022), https://doi.org/10.1016/j.microc.2022.107427.
[12] E. Yüzer, V. Doğan, V. Kılıç, M. Şen, Smartphone embedded deep learning approach for highly accurate and automated colorimetric lactate analysis in sweat, Sens Actuators B Chem. 371 (2022), 132489, https://doi.org/10.1016/j.snb.2022.132489.
[13] T. Hang, S. Xiao, C. Yang, X. Li, C. Guo, G. He, B. Li, C. Yang, H.Jiuan Chen, F. Liu, S. Deng, Y. Zhang, X. Xie, Hierarchical graphene/nanorods-based H2O2 electrochemical sensor with self-cleaning and anti-biofouling properties, Sens Actuators B Chem. 289 (2019) 15–23, https://doi.org/10.1016/j.snb.2019.03.038.
[14] P. Jolly, A. Miodek, D.K. Yang, L.C. Chen, M.D. Lloyd, P. Estrela, Electro-engineered polymeric films for the development of sensitive aptasensors for prostate cancer marker detection, ACS Sens. 1 (2016) 1308–1314, https://doi.org/10.1021/acssensors.6b00443.
[15] Q. Song, R. Zhao, T. Liu, L. Gao, C. Su, Y. Ye, S.Y. Chan, X. Liu, K. Wang, P. Li, W. Huang, One-step vapor deposition of fluorinated polycationic coating to fabricate antifouling and anti-infective textile against drug-resistant bacteria and viruses, Chem. Eng. J. 418 (2021), https://doi.org/10.1016/j.cej.2021.129368.
[16] D.W. Wei, H. Wei, A.C. Gauthier, J. Song, Y. Jin, H. Xiao, Superhydrophobic modification of cellulose and cotton textiles: methodologies and applications, J. Bioresour. Bioprod. 5 (2020) 1–15, https://doi.org/10.1016/j.jobab.2020.03.001.
[17] J.D. Brassard, D.K. Sarkar, J. Perron, Fluorine based superhydrophobic coatings, Appl. Sci. 2 (2012) 453–464, https://doi.org/10.3390/app2020453.
[18] S. Gorji Kandi, M. Amani Tehran, M. Rahmati, Colour dependency of textile samples on the surface texture, Color. Technol. 124 (2008) 348–354, https://doi.org/10.1111/j.1478-4408.2008.00162.x.

[19] J.H. Xin, H.L. Shen, C.C. Lam, Investigation of texture effect on visual colour difference evaluation, Color Res. Appl. 30 (2005) 341–347, https://doi.org/10.1002/col.20138.
[20] S.G. Kandi, M.A. Tehran, Investigating the effect of texture on the performance of color difference formulae, Color Res. Appl. 35 (2010) 94–100, https://doi.org/10.1002/col.20555.
[21] A.C. Akşit, N. Onar, Leaching and fastness behavior of cotton fabrics dyed with different type of dyes using sol-gel process, J. Appl. Polym. Sci. 109 (2008) 97–105, https://doi.org/10.1002/app.27284.
[22] R. Fan, J. Du, K.W. Park, L.H. Chang, E.R. Strieter, T.L. Andrew, Immobilization of nanobodies with vapor-deposited polymer encapsulation for robust biosensors, ACS Appl. Polym. Mater. 3 (2021) 2561–2567, https://doi.org/10.1021/acsapm.1c00140.
[23] K. Khachornsakkul, K.H. Hung, J.J. Chang, W. Dungchai, C.H. Chen, A rapid and highly sensitive paper-based colorimetric device for the on-site screening of ammonia gas, Analyst 146 (2021) 2919–2927, https://doi.org/10.1039/d1an00032b.
[24] J. Trepte, H. Böttcher, Improvement in the leaching behavior of dye-doped modified silica layers coated onto paper or textiles, J. Solgel Sci. Technol. 19 (2000) 691–694, https://doi.org/10.1023/A:1008766807514.
[25] P. Montméat, J. Dechamp, G. Enyedi, F. Fournel, Z. Zavvou, V. Jousseaume, Initiated chemical vapor deposition of polysiloxane as adhesive nanolayer for silicon wafer bonding, Mater. Sci. Semicond. Process 148 (2022), https://doi.org/10.1016/j.mssp.2022.106808.
[26] K. Unger, F. Greco, A.M. Coclite, Temporary tattoo pH sensor with pH-responsive hydrogel via initiated chemical vapor deposition, Adv. Mater. Technol. 7 (2022) 1–12, https://doi.org/10.1002/admt.202100717.
[27] R. Fan, T.L. Andrew, Biosensor encapsulation via photoinitiated chemical vapor deposition (piCVD), J. Electrochem. Soc. 168 (2021), 077518, https://doi.org/10.1149/1945-7111/ac1705.
[28] B. Şimşek, M. Karaman, Initiated chemical vapor deposition of poly (hexafluorobutyl acrylate) thin films for superhydrophobic surface modification of nanostructured textile surfaces, J. Coat. Technol. Res. 17 (2020) 381–391, https://doi.org/10.1007/s11998-019-00282-7.
[29] E.W. Abrahamson, J.G.F. Littler, K.P. Vo, Spectroscopic basis of carbonyl photochemistry. I. The role of excited-state geometry in the photodecomposition of formaldehyde, J. Chem. Phys. 44 (1966) 4082–4086, https://doi.org/10.1063/1.1726586.
[30] A. Forner-Cuenca, V. Manzi-Orezzoli, J. Biesdorf, M. el Kazzi, D. Streich, L. Gubler, T.J. Schmidt, P. Boillat, Advanced water management in PEFCs: diffusion layers with patterned wettability, J. Electrochem. Soc. 163 (2016) F788–F801, https://doi.org/10.1149/2.0271608jes.
[31] N.J. Olsavsky, V.M. Kearns, C.P. Beckman, P.L. Sheehan, F.J. Burpo, H. D. Bahaghighat, E.A. Nagelli, Review research and regulatory advancements on remediation and degradation of fluorinated polymer compounds, Appl. Sci. 10 (2020) 1–26, https://doi.org/10.3390/app10196921.
[32] M. Zahid, T. Khalid, Z.A. Rehan, T. Javed, S. Akram, A. Rashid, S.K. Mustafa, R. Shabbir, F. Mora-Poblete, M.S. Asad, R. Liaquat, M.M. Hassan, M.A. Amin, H. A. Shakoor, Fabrication and characterization of sulfonated graphene oxide (Sgo) doped pvdf nanocomposite membranes with improved anti-biofouling performance, Membranes 11 (2021), https://doi.org/10.3390/membranes11100749.
[33] S. Li, P. Huang, Z. Ye, Y. Wang, W. Wang, D. Kong, J. Zhang, L. Deng, A. Dong, Layer-by-layer zwitterionic modification of diverse substrates with durable anti-corrosion and anti-fouling properties, J. Mater. Chem. B 7 (2019) 6024–6034, https://doi.org/10.1039/c9tb01337g.
[34] E. Molena, C. Credi, C. de Marco, M. Levi, S. Turri, G. Simeone, Protein antifouling and fouling-release in perfluoropolyether surfaces, Appl. Surf. Sci. 309 (2014) 160–167, https://doi.org/10.1016/j.apsusc.2014.04.211.
[35] P. Krishnamoorthy, P. Sathyadevi, P.T. Muthiah, N. Dharmaraj, Nickel and cobalt complexes of benzoic acid (2-hydroxy-benzylidene)- hydrazide ligand: Synthesis, structure and comparative in vitro evaluations of biological perspectives, RSC Adv. 2 (2012) 12190–12203, https://doi.org/10.1039/c2ra20597a.
[36] A.J. Rodríguez, C.R. Zamarreño, I.R. Matías, F.J. Arregui, R.F.D. Cruz, D.A. May-Arrioja, A fiber optic ammonia sensor using a universal pH indicator, Sensors 14 (2014) 4060–4073, https://doi.org/10.3390/s140304060.